Chapter 3
Existing Buildings: The New Italian Provisions for Probabilistic Seismic Assessment

Paolo Emilio Pinto and Paolo Franchin

Abstract In Europe, the reference document for the seismic assessment of buildings is the Eurocode 8-Part3, whose first draft goes back to 1996 and, for what concerns its safety format, has strong similarities with FEMA 276. Extended use of this document, especially in Italy after the 2009 L'Aquila earthquake has shown its inadequacy to provide consistent and univocal results. This situation has motivated the National Research Council of Italy to produce a document of a level higher than the one in force, characterized by a fully probabilistic structure allowing to account for all types of uncertainties and providing measures of performance in terms of mean rates of exceedance for a selected number of Limit States (LS). The document, which covers both reinforced concrete and masonry buildings, offers three alternative approaches to risk assessment, all of them belonging to the present consolidated state of knowledge in the area. These approaches include, in decreasing order of accuracy: (a) Incremental dynamic analysis on the complete structural model, (b) Incremental dynamic analysis on equivalent SDOF oscillator(s), (c) Non-linear static analysis. In all three approaches relevant uncertainties are distinguished in two classes: those amenable of description as continuous random variables and those requiring the set-up of different structural models. The first ones are taken into account by sampling a number of realizations from their respective distributions and by associating each realization with one of the records used for evaluating the structural response, the latter by having recourse to a logic tree. Exceedance of each of the three considered Limit States: Light or Severe damage and Collapse, is signaled by a scalar indicator Y, expressing the global state of the structure as a function of that of its members, taking a value of one when the Limit State is reached. For the first two LS's, which relate to functionality and to economic considerations, the formulation of Y is such as to leave to the owner the choice of the acceptable level of damage, while

P.E. Pinto (✉) • P. Franchin
Department of Structural and Geotechnical Engineering, University of Rome La Sapienza, Via Antonio Gramsci 53, 00197 Rome, Italy
e-mail: profpaolopinto@gmail.com; paolo.pinto@uniroma1.it; paolo.franchin@uniroma1.it

A. Ansal (ed.), *Perspectives on European Earthquake Engineering and Seismology*, Geotechnical, Geological and Earthquake Engineering 34,
DOI 10.1007/978-3-319-07118-3_3,

for the Collapse LS the formulation is obviously unique. An application to a real school building completes the paper.

3.1 Preamble

In spite of the availability (officially since 2005, but with preliminary versions since 1996) of Eurocode 8 Part3 (EC8/3) dealing with seismic assessment and retrofitting of buildings, the relevance for Italy of a document of this type had escaped the attention of both the authorities and the profession until a small earthquake occurred in 2002 caused the complete collapse of a school and the death of all the young students inside. This fact produced a national scandal and the awakening in the general public of the consciousness of the seismic risk potentially affecting all types of constructions, the old as well as the recent ones.

The situation prompted the Department of Civil Protection to take action in two directions: preparing a technical document dealing with the analytical seismic assessment of buildings, and emanating an ordnance requiring that all important public facilities be subjected to assessment within 5 years time. The technical document can be regarded essentially as the translation of the EC8/3: it has been made official in 2008 by the competent Ministry (NTC2008) Ministero Infrastrutture (2008) and its use mandatory in July 2009, right after the April 6th 2009 L'Aquila earthquake.

3.1.1 The Present Normative State and the Purpose of the New Document Issued by the National Research Council

It will be understood that due to the ordnance of 2003 a very large number of buildings has been by now subjected to seismic assessment using basically EC8/3, so that experience on its merits and limitations rests on solid statistical bases. Critical aspects have emerged from the use of EC8/3, not only in Italy, but in a number of other European Countries as well, and plans for an improved version are under way. The consensus existing on major critical aspects allows for just a brief mention to be made here.

(a) Performance must be checked with reference to three Limit States. These are formulated in terms of system performance, but then the verifications, for reinforced concrete (RC) buildings, must be carried out in terms of member behavior, independently of the number and the importance of non-complying members. This inconsistency is a major cause of dispersion of the results obtained by different analysts.

(b) The uncertainties regarding the structure are grouped into three types, namely: those related to geometry, to the properties of the materials and to the details of reinforcement (for RC structures.) Three levels of knowledge are considered, each one characterized by a combination of the knowledge acquired on the three types of uncertainty, and a so-called "confidence factor (CF)" is associated to each level. In many cases in practice, however, the achievable state of knowledge does not fit in any of the levels above, due to non-uniform quality/quantity of information on the three aspects, with the consequent uncertainty on the value of CF to be adopted.
(c) The CF factors are to be applied to the material properties, which are only one of the many sources of uncertainties, and in the majority of cases are of comparatively much lesser relevance on the outcome of the assessment.
(d) Little if any guidance is given on the modeling of the structure, e.g. on the use of classical fiber elements or of stiffness/strength degrading models. Yet different choices on these aspects are rather consequential on the definition of the attainment of the LS's, especially for that of collapse.

In consideration of the above mentioned limits, the National Research Council (CNR) decided to prepare a document of a level higher than the one in force, in which the performance-based concept, which is claimed to be at the base of most of the modern design codes, is implemented in explicit probabilistic terms, allowing thus uncertainties of all nature to be taken into consideration and introduced into the assessment process, with their relevance on the final outcome properly reflected.

For what concerns the probabilistic procedures adopted the choice has been to adhere to the now well consolidated state-of–the-art, avoiding refinements deemed as inessential, in order to make the document accessible to a larger audience.

The CNR documents, denominated "Instructions", do not have the status of "state laws", as it is the case for the Ministerial norms, so they cannot replace or contrast with the latter, but they enjoy a high scientific reputation, and recourse to them is frequent in case of dubious or absent indications in the norms. It is auspicable and plausible that the future revision of the norms will take profit of both the format as well of the content of the new document.

3.1.2 The Content of the CNR Instructions

The main content of the document is subdivided into the following chapters.

1. Introduction
2. Methodological aspects common to all typologies:
   - Limit States
   - Target performances
   - Seismic action
   - Knowledge acquisition

- Uncertainty modeling
- Structural analysis
- Identification of LS exceedance
- Assessment methods.

3. Specific provisions for masonry buildings
   - Response modeling
   - Probabilistic capacity models
4. Specific provisions for reinforced concrete buildings
   - Response modeling
   - Probabilistic capacity modeling
5. Commentary to the text
6. Example application to a masonry building
7. Example application to a reinforced concrete building

The present paper illustrates all material devoted to reinforced concrete buildings.

3.2 Methodological Aspects Common to All Typologies

3.2.1 Limit States

The Limit States are defined with reference to the performance of the building in its entirety including, in addition to the structural part, also non-structural ones like partitions, electrical and hydraulic systems, etc.

The following three Limit States are considered:

- Damage Limit State (SLD): negligible damages (no repair necessary) to the structural parts, and light, economically repairable damages to the non-structural ones.
- Severe Damage (also called life safeguard) Limit State (SLS): loss of use of non-structural systems and a residual capacity to resist horizontal actions. State of damage uneconomic to repair.
- Collapse prevention Limit State (SLC): the building is still standing but would not survive an aftershock.

Check against the attainment of the SLC is mandatory, in consideration of the general lack of reserve ductility of non-seismically designed buildings (contrary to the proven large reserve possessed by buildings designed according to present seismic codes).

Table 3.1 Minimum levels of protection in terms of maximum tolerated λ_{LS} (values in the table are multiplied by 10^3) as a function of building class

Limit state	Class I	Class II	Class III	Class IV
SLD	64.0	45.0	30.0	22.0
SLS	6.8	4.7	3.2	2.4
SLC	3.3	2.3	1.5	1.2

3.2.2 Target Performances

A distinction is made among buildings depending on the socio-economic consequences of their LS exceedance, and four Classes of importance are identified.

The required level of protection for each Class and each Limit State is formulated in terms of the mean annual frequency of exceedance (MAF): λ_{LS}.

The proposed maximum values of λ_{LS} are such as to ensure approximately the same level of protection as currently required by the national seismic code for the different Classes and LS's for new buildings. They are reported in Table 3.1.

The values in the table have been calculated using the approximate expression due to Cornell et al. (2002):

$$\lambda_{LS} = \lambda_S\left(S_{\hat{D}=\hat{C}}\right)\exp\left|\frac{1}{2}\frac{k_1^2}{b^2}\left(\beta_D^2+\beta_C^2\right)\right| \tag{3.1}$$

expressing the MAF of the LS as the MAF of the seismic intensity inducing a median demand equal to the median capacity, times an amplification factor accounting for the uncertainty in demand β_D and capacity β_D, as well as the slopes of the hazard curve k_1 and of the intensity – demand relation b. If the common values $k_1 = 3$, $b = 1$, $\beta_D = \beta_D = 0.3$ are introduced, the exponential factor takes the value ~2.25. Taking for $\lambda_S\left(S_{\hat{D}=\hat{C}}\right)$ the inverse of the mean return period T_R of the seismic action to be considered for each Class and LS in the current deterministic code, leads to $\lambda_{LS}^* = 2.25/T_R$, which corresponds e.g. for Class II buildings (ordinary) and the severe damage LS to: $2.25/475 = 0.0047$.

3.2.3 Seismic Action

In line with the adopted IM-based approach, the seismic action is characterized in terms of:

- the mean hazard curve for the site
- a set of time histories of the seismic motion, used for the calculation of the fragility $p_{LS}(s)$

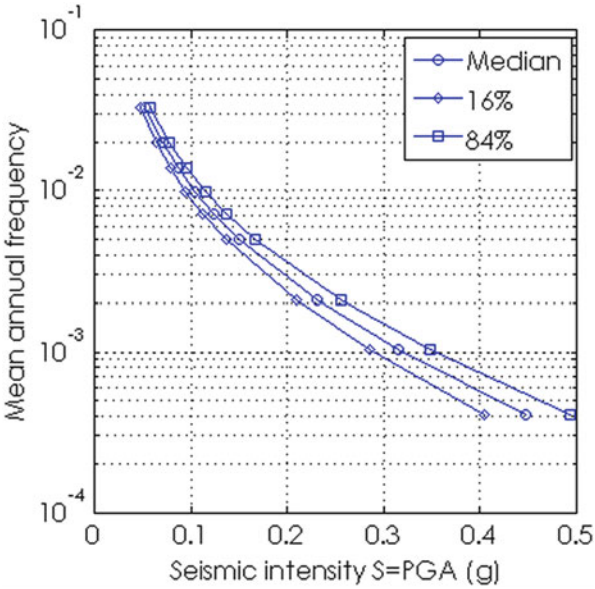

Fig. 3.1 Median and 16 %/ 84 % fractile hazard curves

A discrete hazard curve (Fig. 3.1) for any site in Italy can be obtained from the *median* uniform hazard spectra (UHS) provided in the national code for nine values of the mean return periods, ranging from 30 to 2,475 years. The UHS are provided at the nodes of a square grid with sides of about 5 km. The hazard in a point inside a grid is obtained by interpolation of the values at its four corners.

For any given value T of the structural period the nine values of $S_a(T)$ provide a point-wise median hazard curve to which, for the purpose of the evaluation of λ_{LS}, a quadratic interpolation function is applied.

As suggested in the SAC-FEMA procedure (Cornell et al. 2002), the epistemic uncertainty on the hazard curve is accounted for by using its mean value, instead of the median, which is obtained by multiplying the latter by an amplification factor:

$$\overline{\lambda}(s) = \lambda_{S,50\%}(S)\exp\left(\frac{1}{2}\beta_H^2\right) \tag{3.2}$$

where the uncertainty on the hazard is:

$$\beta_H = \sigma_{\ln S} = \frac{\ln S_{84\%} - \ln S_{16\%}}{2} \tag{3.3}$$

The above expression is obtained assuming a lognormal distribution for the intensity S at any given λ_S, and the uncertainty should be evaluated at the intensity with MAF close to λ_{LS} (an iteration is therefore required).

The time histories to be used for response analysis can be either natural records or artificially generated motions, provided these latter are able to reproduce the same mean, variance and correlation of the spectral ordinates of the natural motions.

The selection of the natural records can be made, according to the state of the practice, using the technique of disaggregation of the hazard in terms of magnitude M, distance R and epsilon: it is suggested that the above data are obtained for values of the IM characterized by a MAF in the interval from 1/500 to 1/2,000. The use of more refined techniques for record selection is also allowed (Bradley 2013; Lin et al. 2013).

The minimum number of motions is 30.

The selection of the records should be made among those recorded on rock or stiff soil. If the site is characterized by soft soil (e.g. V_{s30} in the interval 180–360 m/s, or less) a site response analysis is mandatory. Equivalent linear methods can be used for this purpose if significant inelastic response at the higher intensities is not expected, otherwise fully non-linear methods must be employed.

Uncertainties regarding soil profile and geotechnical parameters should be treated in the same way as those related to the structure above soil, see 3.2.5).

For sites in proximity of known active faults the probability of occurrence of pulse-like motions must be evaluated and the selection of records should proportionately reflect it.

3.2.4 Knowledge Acquisition

Given that a fully exhaustive (i.e. deterministic) knowledge of an existing building in terms of geometry, detailing and properties of the materials is realistically impossible to achieve, it is required that every type of incomplete information be explicitly recognized and quantified, for introduction in the assessment process in the form of additional random variables or of alternative assumptions. Since the number and the relevance of the considered uncertainties has an obvious bearing on the final evaluation of the risk, and consequently on the cost of the upgrading intervention, the search for a balance between the cost for additional information and the potential saving in the intervention should be a guiding criterion in the knowledge acquisition process.

Based on the above consideration the provisions do not prescribe quantitative minima for the number of elements to be inspected, the number of samples to be taken, etc. They ask instead for a sensitivity analysis to be carried out on one or more preliminary models of the building (variations on a first approximation of the final model). For RC structures this analysis is of the linear dynamic type (modal with full elastic response spectrum), which is adequate to expose global modes of response (regular or less regular) and to provide an estimate of the member chord rotations demands to be compared with yield chord rotation capacities. The latter, being quite insensitive to the amount of reinforcement, can be obtained based on gross concrete dimensions and nominal steel properties. The results of these analyses would then provide guidance on where to concentrate tests and inspections.

The extension of these tests depends on the initial amount of information. If original construction drawings are available, only limited verification of the actual reinforcement details is required, through concrete removal over an area sufficient to expose longitudinal and transverse reinforcement (and estimate spacing). When drawings are incomplete or missing, the extension of test/inspections must increase to understand the "designer's modus operandi" in view of replicating it (this is regarded as more effective than blindly applying the ruling provisions at the time in a simulated design).

3.2.5 Uncertainty Modeling

All types of uncertainties are assumed to belong to either one of the following two classes:

- those describing variations of parameters within a single model, amenable to a description in terms of random variables, with their associated distribution function
- those whose description requires consideration of multiple models, to each of which a subjective mass probability function is associated.

The uncertainties belonging to the first class include: the seismic intensity at the site, governed by the hazard function, the record-to record variability, described by a set of records, all material properties, related both to the soil and to the structure, normally described as lognormal variables, and the model error terms of the capacity models, also usually described as lognormal variables.

The uncertainties belonging to the second class include, among others, the geometry of the structure (e.g. presence and dimension of certain elements whose precise identification would be too invasive), the reinforcement details in important places, alternative models for the capacity of the elements, alternative models for the behavior of the components (e.g. degrading or non degrading).

Uncertainties of this class are treated with the logic tree technique, where mass probabilities are assigned to the alternative assumptions for each of uncertain factor. The concept is illustrated in Fig. 3.2 in which the alternative assumptions are made at each node, and the result obtained with any particular sequence of assumptions (the branches of the tree) is weighted by the product of the mass probabilities assigned to the each of them, due to the assumed independence of the factors (X, Y and Z in the figure).

3.2.6 Structural Analysis and Modeling

Exclusive recourse to non-linear methods of analysis, accounting for material and geometric non-linear phenomena, is considered in the provisions. The analysis can

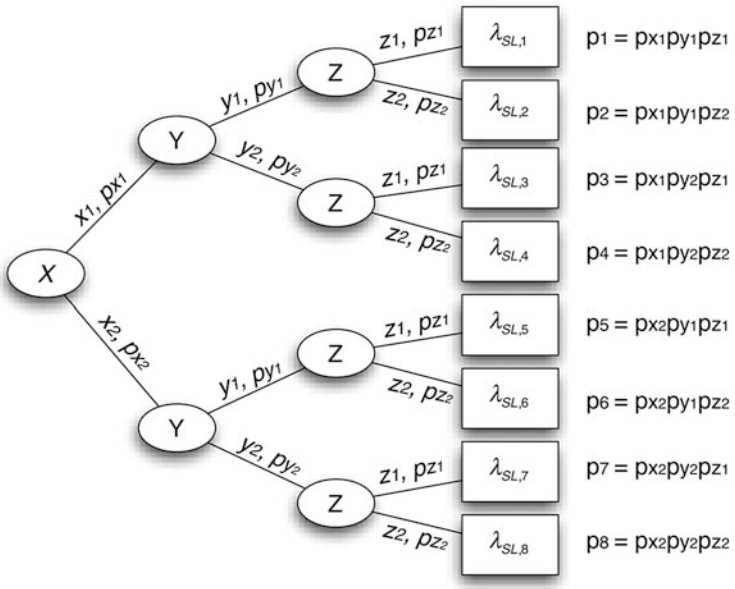

Fig. 3.2 Logic tree

be either static or dynamic, and guidance is given for the application, as it will be illustrated in the following (recall that for reason of space this paper covers only the part relative to RC buildings, the part devoted to masonry buildings is at least equivalent in terms of extension and detail).

The structural model must be tri-dimensional, with simultaneous excitation applied along two orthogonal directions.

Regarding the behavior of the structural members (beams and columns) under cyclic loading of increasing amplitude two modeling approaches are considered, as shown in Fig. 3.3.

- Non-degrading, i.e. stable hysteretic behavior without degradation of strength but overall degradation of stiffness (Takeda-type models)
- Degrading, where both stiffness and strength degrade with increasing cyclic amplitude down to negligible values.

The document provides in Chap. 4 an overview of the state of the art on this latter type of models for RC structures.

It is important to note from now that the use of the two different types of models has important reflexes in the identification of the collapse limit state of the structure.

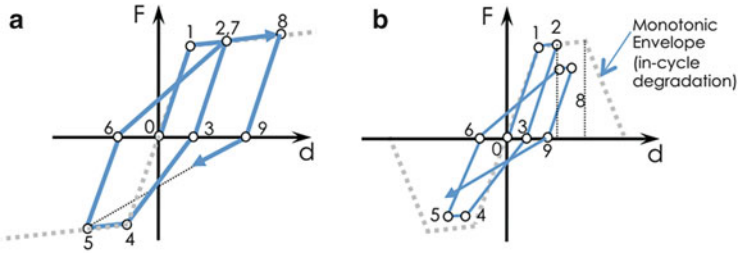

Fig. 3.3 Non-degrading (**a**) vs degrading (**b**) nonlinear modeling

3.2.7 Identification of LS Exceedance

Exceedance of each LS is signaled by a scalar indicator Y, expressing the global state of the structure as a function of that of its members, taking a value equal or larger than unity. Its definition depends on the considered LS. For the first two LS's, of light and severe damage, which pertain functionality and economic feasibility of repair actions, the choice of an appropriate threshold is left to the analyst in accordance to the owner/stakeholder requirements. The formulation of Y for the collapse limit state, related to safety, is stricter and does not leave space for subjective choices on the analyst side.

3.2.7.1 Light Damage

For the purpose of the identification of the light damage LS, the building is considered as composed by N_{st} structural members and N_{nst} non-structural components:

$$Y_{SLD} = \frac{1}{\tau_{SLD}} \max \left[\sum_{i=1}^{N_{st}} w_i I\left(\frac{D_i}{C_{i,SLD}}\right); \sum_{j=1}^{N_{nst}} w_j I\left(\frac{D_j}{C_{j,SLD}}\right) \right] \tag{3.4}$$

In the above expression, D and C indicate the appropriate demand and capacity values, I is an indicator function taking the value of one when $D \geq C$ and zero otherwise, and the w's are weights summing up to one, accounting for the importance of different members/components. The indicator Y attains unity when the max function equals τ_{SLD}, a user-defined tolerable maximum cumulative damage. (e.g. something in the range 3–5 %).

3.2.7.2 Severe Damage

For the purpose of the identification of the severe damage LS, the indicator Y is formulated in terms of a conventional total cost of damage to structural and non-structural elements as:

$$Y_{SLS} = \begin{cases} \dfrac{1}{\tau_{SLS}} \left[\alpha_{st} \sum_{i=1}^{N_{st}} w_i c \left(\dfrac{D_i}{C_{i,SLS}} \right) + (1 - \alpha_{st}) \sum_{j=1}^{N_{nst}} w_j c \left(\dfrac{D_i}{C_{j,SLS}} \right) \right] \text{if } Y_{SLC} < 1 \\ 1 \text{ if } Y_{SLC} \geq 1 \end{cases} \tag{3.5}$$

where α_{st} is the economic "weight" of the structural part (i.e. about 20 % in a low- to mid-rise residential building); $c(D/C)$ is a conventional cost function which starts from zero for $D = 0$ and reaches unity, i.e. the replacement cost for the element, for $D = C_{SLS}$ (with C_{SLS} usually a fraction of the ultimate capacity of the element); as for the light damage LS, the indicator function attains unity when the quantity within square brackets equals τ_{SLS}, a user-defined fraction of the total building value over which repair is considered economically not competitive with demolition and replacement. Obviously if collapse occurs Y_{SLS} is set to 1.

3.2.7.3 Collapse

As anticipated, the identification of this LS depends on the modeling choices (see §2.6).

If non-degrading elements are adopted, the system is described as a serial arrangement of a number of elements in parallel, so that the Y variable takes the expression (Jalayer et al. 2007):

$$Y_{SLC} = \max_{i=1,N_s} \min_{j \in 1_i} \frac{D_j}{C_{j,SLC}} \tag{3.6}$$

where N_S is the number of parallel sub-systems (cut-sets) in series, and I_i is the sets of indices identifying the members in the i-th sub-system. This formulation requires the a priori identification of the cut-sets. Carrying out this task is in general not immediate, since the critical cut-set depends on the dynamic response and changes from record to record.

If all elements are of the "degrading" type, i.e. they are able to simulate all types of failure, accounting for the interaction of bending and shear, the collapse state $Y = 1$ is identified with the occurrence of the so-called "dynamic instability", that is, when the curve intensity-response becomes almost flat. In order to identify the point on the curve corresponding to $Y = 1$ one can use the expression:

$$Y_{SLC} = (1 + \Delta) - \frac{S'}{S'_0} \text{with } 0 < S' < S'_0 \tag{3.7}$$

with values for Δ in the interval 0.05–0.10, corresponding to a small residual positive stiffness, in order to avoid numerical problems.

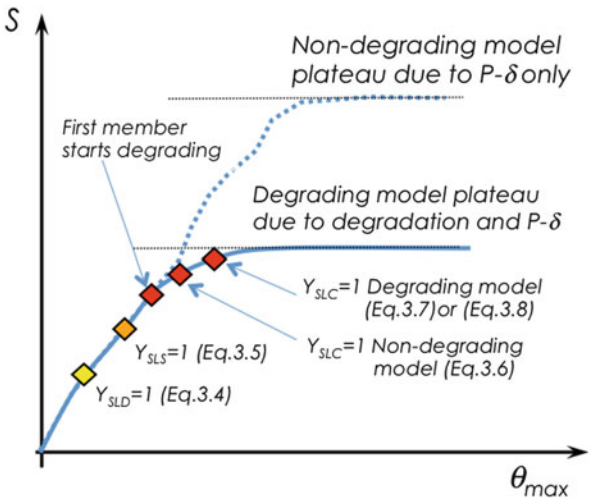

Fig. 3.4 Intensity vs response curve (also known as IDA curve, see 3.2.8.1), as a function of modeling choices

Finally, if the elements are of the degrading type but the adopted formulation cannot account for all possible collapse modes, the indicator variable can be expressed as:

$$Y_{SLC} = \max\left[(1+\Delta) - \frac{S'}{S'_0}; \max_{nsm}\left(\frac{D}{C}\right)\right] \tag{3.8}$$

which simply indicates that the collapse condition is attained for the most unfavorable between dynamic instability and the series of the "non simulated (collapse) modes". Typically, this set includes the axial failure of columns. Care should be taken in selecting the columns to be included in the evaluation of (3.8), limiting it only to those that can really be associated with a partial/global collapse.

The Fig. 3.4 shows an idealized intensity-response relation S vs θ_{max} (maximum interstorey drift ratio), with marks on the points corresponding to LS's according to the above definitions.

3.2.8 Assessment Methods

As already indicated in 3.2.2, the outcome of the assessment is expressed in terms of the mean annual frequency of exceeding any of the proposed three Limit States: λ_{LS}. Differently formulated or additional Limit States could be considered without any modification of the procedure.

The mean annual frequency is obtained using the Total Probability Theorem, as the integral of the product of the probability of exceedance of the LS conditional to the value $S = s$ of the seismic intensity (denominated as "fragility"), times the

probability of the intensity being in the neighborhood of s. This latter is given by the absolute value of the differential of the hazard function at $S = s$:

$$\lambda_{LS} = \int_0^{\infty} p_{LS}(S)|d\lambda_S(S)| \tag{3.9}$$

The integral can be evaluated numerically. However, if the hazard is approximated with a quadratic fit in the log-log plane ($\ln\lambda_S = \ln k_0 + k_1 \ln s + k_2 \ln^2 s$), and the fragility function is assumed to have a lognormal shape, closed forms for the evaluation of the integral are available.

The lognormal assumption is indeed adopted in the provisions based on the international general consensus. The fragility thus takes the form:

$$p_{LS}(S) = p(Y_{LS} \geq 1|S = s) = p(S_{Y_{LS}=1} \leq s) = \Phi\left(\frac{\ln s - \mu_{\ln S_{Y=1}}}{\sigma_{\ln S_{Y=1}}}\right) \tag{3.10}$$

requiring evaluation of two parameters only: the mean and the standard deviation of the logarithm of the seismic intensity inducing the unit value of the Limit State indicator: Y = 1.

The document provides three alternative methods, indicated in the following as A, B and C, for the evaluation of the fragility. All methods require a 3D model of the structure.

3.2.8.1 Method A: Incremental Dynamic Analysis on the Complete Model

Recourse is made to the well known technique usually referred to as Incremental Dynamic Analysis (IDA) (Vamvatsikos and Cornell 2002): it consists in subjecting the complete 3D model of the structure to a suite of n time-histories (each with two orthogonal horizontal components, the vertical component being normally omitted in case of ordinary buildings), each time-history being scaled at increasing intensity levels. At each level of S the value of Y is calculated, and the set of (S,Y) points are plotted to obtain a curve in the intensity-response plane, denoted as "IDA" curve.

A sample of values of S leading to Y = 1 is obtained from the set of n IDA curves, as shown in Fig. 3.5, left: this sample is used to evaluate the parameters $\mu_{\ln S_{Y=1}}$ and $\sigma_{\ln S_{Y=1}}$.

The effect of the uncertainties that can be modeled as continuous can be approximately determined by associating to each ground motion a sample of the uncertainties taken from their distributions (the approach is acceptable if the number of time-histories is adequate to describe at least approximately the distribution of the r.v.'s). The effect of the introduction of the uncertainties is visible on the IDA curves by their larger spread (Fig. 3.5, right).

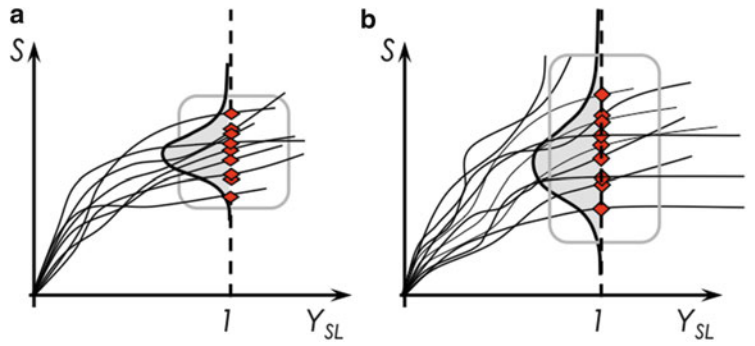

Fig. 3.5 IDA curves and samples of the SY = 1 intensity values: (**a**) including record-to-record variability only, (**b**) with structural uncertainty

3.2.8.2 Method B: Incremental Dynamic Analysis on an Equivalent Single Degree-of-Freedom Oscillator

This method differs from the previous one for the fact that the incremental dynamic analyses are carried out on a (number of) "equivalent" single degree–of–freedom (SDOF) oscillators, obtained through nonlinear static (NLS) analysis on the 3D model. Any of the available types of NLS analysis can be adopted, as appropriate for the case at hand.

The global curve relating base shear to the top displacement obtained from the pushover becomes the force-displacement relationship of a simple oscillator, which for the purpose of the response analysis is approximated with a multi-linear relationship.

The number of the needed SDOF oscillators equals the number of modes contributing significantly to the total 3D response. On each SDOF an IDA analysis is performed for all of selected time-histories: for any time-history, modal responses, obtained translating the maximum dynamic response of each SDOF in the response of the 3D structure, at the same intensity level are combined by an appropriate rule (SRSS or CQC) to yield the total response. The latter is used to compute the indicator variable for each LS. Then collection of $S_{Y=1}$ values and evaluation of the fragility parameters $\mu_{\ln S_{Y=1}}$ and $\sigma_{\ln S_{Y=1}}$ proceeds as per method A.

The effect of the uncertainties that can be modeled as continuous can be treated in the same approximate way as in Method A. In this case the pushover analyses must be repeated on different structures each one characterized by a different realization of the uncertainties, and associated one-to-one with the selected motions.

3.2.8.3 Method C: Non-linear Static Analysis and Response Surface

This method is again based on nonlinear static analysis. The main differences with respect to method B are two: demand on the SDOF oscillators is determined using the response spectra of the selected time-histories (the actual response can be obtained using any of the available methods for obtaining the inelastic displacement response from an elastic spectrum), and the effect of the system-related uncertainties that can be modeled as continuous is determined through the use of the Response Surface technique (Pinto et al. 2004).

The two parameters of the fragility function are determined as follows.

The log-mean is obtained from the median response spectrum of the selected time-histories (scaled to the same S=s), whose intensity is scaled upwards until $Y = 1$ is obtained:

$$\mu_{\ln S_{Y=1}} = \ln S_{Y=1}\big|_{S_{a,50\%}(T)} \tag{3.11}$$

The logarithmic standard deviation is assumed as independently contributed by two factors: the variability of the response due to the variability of the ground motions (given $S = s$), and the variability due to the randomness of the material properties:

$$\sigma_{\ln S_{Y=1}} = \sqrt{\sigma^2_{\ln S_{Y=1},S} + \sigma^2_{\ln S_{Y=1},C}} \tag{3.12}$$

The first of the two terms is evaluated from the response spectra fractiles at 16 and 84 % from the selected time-histories (scaled to the same S=s) according to:

$$\sigma_{\ln S_{Y=1},S} = \frac{\ln S_{Y=1|16\%} - \ln S_{Y=1|84\%}}{2} \tag{3.13}$$

The influence on $S_{Y=1}$ of the continuous random variables, denoted by X_k, is studied by expressing $\ln S_{Y=1}$ as a linear response surface, in the space of the normalized variables $x_k = (X_k - \mu_{Xk})/\sigma_{Xk}$:

$$\ln S_{Y=1} = \alpha_0 + \sum_k \alpha_k x_k + \varepsilon \tag{3.14}$$

The normalized variables are assigned the values ± 1 in correspondence of their fractile values of 16 % and 84 %. The N parameters α_k are obtained through a complete factorial combination of the variables at two levels (+1,−1). For each of the $M = 2^N$ combinations the median spectrum is increased up to the value producing $Y = 1$. The values attributed to the normalized variables (+1or −1) for each of the combinations are the rows of a so-called "matrix of experiments" **Z**, and the corresponding values of $\ln S_{Y=1}$ form a vector of "response" denoted as **y**.

The parameters α_k are then obtained from the expression:

$$\alpha = \left(\mathbf{z}^T\mathbf{z}\right)^{-1}\mathbf{z}^T\mathbf{y} \tag{3.15}$$

from which the component of $\sigma_{\ln S_{Y=1}}$ related to the uncertainty in the structure ("capacity") follows as:

$$\sigma_{\ln S_{Y=1},C} = \sqrt{\sum_k \sum_j \alpha_k \alpha_j \rho_{x_i x_j} + \sigma_\varepsilon^2} \tag{3.16}$$

where σ_ε^2 is the variance of the residuals, and the facts that ε and $\mathbf{x}$ are independent, and the latter are correlated standard variables with correlation coefficient ρ has been used.

3.3 RC Specific Provisions

This chapter complements the general Chap. 2, by providing detailed indications on modeling of response and capacity for RC structures. As mentioned before the document is based exclusively on nonlinear analysis and prescribes a mandatory verification of the collapse LS. Inelastic models that describe response up to collapse, however, are still not in the average technical background of engineers, and, also, they are still evolving toward a more mature and consolidated state. In recognition of this, the document introduces formulations for the identification of the collapse LS that allow a correct use of the mainstream non-degrading models (3.6), but leaves the door open to the use of more advanced degrading models (3.7). Further, in order to guide the user in the selection of the latter, it provides a brief reasoned classification of inelastic response models.

3.3.1 Response Models

Models for beam-columns, joints and masonry infills are presented, though the former are obviously given the major attention. In particular, collapse modes of RC columns are described, as schematically shown in Fig. 3.6. The figure illustrates the possible modes of collapse in a monotonic loading condition, in terms of shear force-chord rotation of the member. In all three cases the plot shows with dashed grey lines the monotonic response in a pure flexural mode, with the usual I, II and III stages up to ultimate/peak strength, followed by a fourth descending branch to actual collapse, and the shear strength envelope. The latter starts with $V_{R,0}$ and decreases as a function of deformation, measured in terms of ductility μ. Depending on whether the two curves cross before flexural yield, after, or do not cross at all, the member fails in brittle shear, ductile shear or flexure. In all cases, collapse occurs

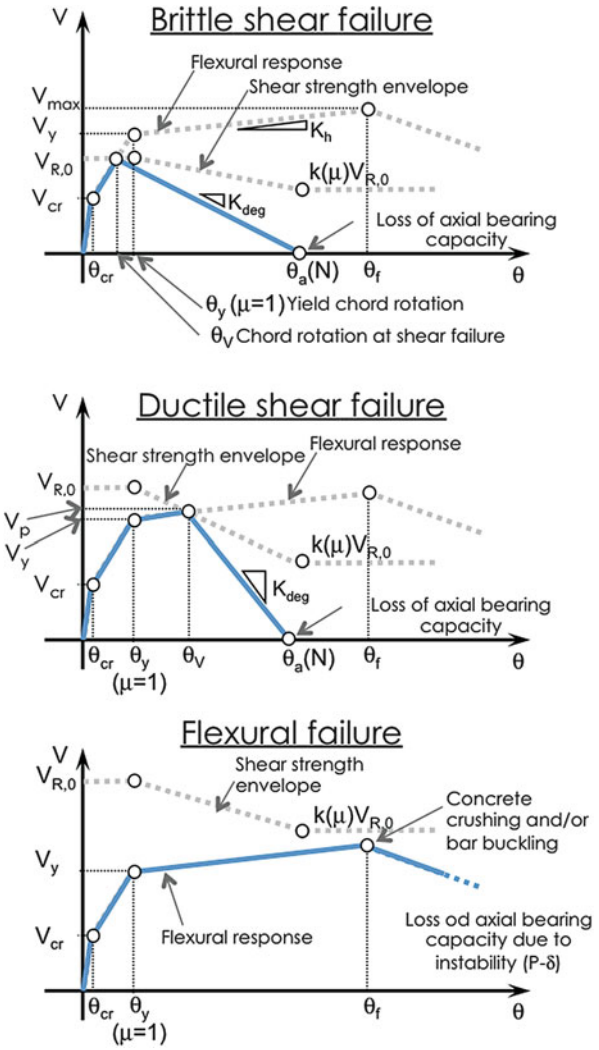

Fig. 3.6 Collapse modes of RC columns (chord rotations at peak strength, usually denoted as ultimate values θ_u, are here differentiated as either shear θ_V or flexural θ_f)

due to loss of vertical load-bearing capacity ($V_R = N_R = 0$) at the end of the degrading branch.

In cyclic loading at large amplitude the response presents a second contribution to degradation, which is cyclic degradation, as shown in Fig. 3.7.

Available models can be classified in mechanical and phenomenological. The state of the art of purely mechanical models is not yet capable of describing the full range of behaviour of RC members illustrated in Figs. 3.6 and 3.7 (especially for brittle and ductile shear collapse). Currently, if the analyst wishes to incorporate degrading models, the only viable option is to use phenomenological (e.g. Ibarra et al. 2005) or hybrid models (Elwood 2004). These models, however, also have

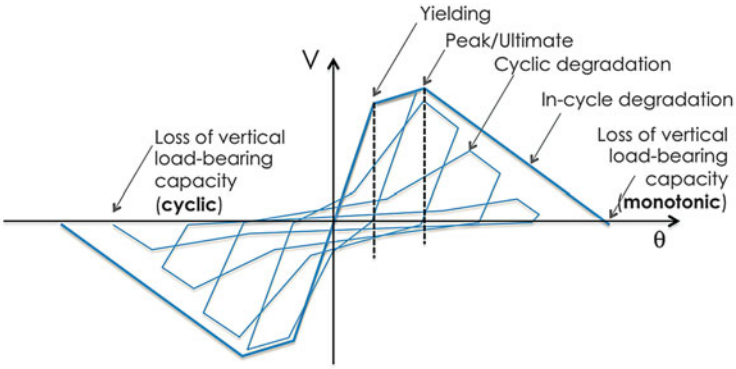

Fig. 3.7 Cyclic and in-cycle components of degradation (Response shown is from Ibarra et al. model)

their limitations and, for instance, rely heavily on the experimental base used to develop them, which is often not large enough (e.g. for the Ibarra et al. model, the proportion of ductile shear and flexural failures dominate the experimental base, resulting in limited confidence on the model capability to describe brittle failures). Further, computational robustness is an issue with all these models.

Figure 3.7 shows the monotonic backbone (e.g. for the ductile shear collapse mode) and the cyclic response. It is important to note that the deformation thresholds corresponding to state transitions and ultimately to collapse are different for monotonic and cyclic loading. This fact is highlighted in Fig. 3.8, where the peak/ultimate and axial failure rotations are clearly identified as different in the monotonic and cyclic loading.

The user is advised that consistency is essential in the choices of response, capacity and LS identification formulas.

If non-degrading models are chosen, one should use (3.6) for collapse identification, with peak deformation thresholds $\theta_{u,cyclic}$ that account on the capacity side for the degradation disregarded on the response side.

If degrading models are used, (3.7) or (3.8) are employed, and the monotonic deformation thresholds, $\theta_{u,mono}$, $\theta_{a,mono}$, etc are used as input parameters for the response model (together with degradation parameters).

3.3.2 Capacity Models

A survey of probabilistic models for the deformation thresholds shown before, grouped by LS, is presented in the document. Requirements for an ideal set of models are stated explicitly: consistency of derivation of thresholds of increasing amplitude (i.e. yield, peak and axial deformation models derived based on the same experimental tests, accounting also for correlations), and an experimental base

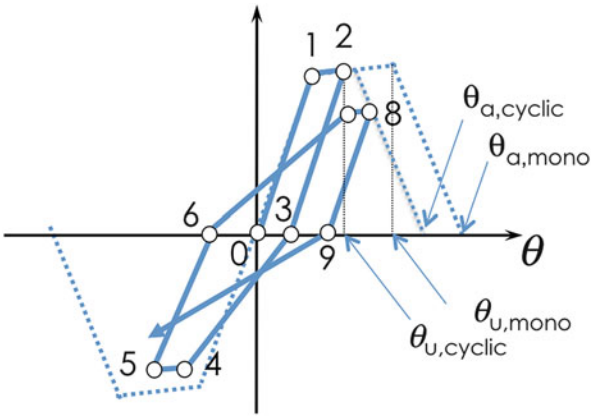

Fig. 3.8 Deformation limits for monotonic and cyclic loading

covering the full range of behaviours (different types of collapse, different reinforcement layouts, etc) in a balanced manner. Such a set of models is currently not available.

One set of models that comes closer to the above requirements, and is used in the application illustrated in the next section, is that by Haselton et al. (2008), which consists of predictive equations for the parameters of the Ibarra et al. (2005) degrading hysteretic model. Haselton et al, however, provide only mean and standard deviation of the logarithm of each parameter, disregarding pair-wise correlation, in spite of the fact that the equations were established on the same experimental basis. Also, as already anticipated, brittle shear failures are not represented.

Figure 3.9 shows the tri-linear moment-rotation monotonic envelope according to the Ibarra model, with qualitative (marginal) probability density functions (PDFs) for its parameters, as supplied by Haselton et al. (2008). Not all the parameters can be independently predicted at the same time, to maintain physical consistency of the moment-rotation law. In the application the stiffness at 40 % and 100 % of yield, and the rotation increment $\Delta\theta_f$ and $\Delta\theta_a$ have been used (darker PDFs in the figure). Use of the latter two in place of θ_f and θ_a ensures that situations with $\theta_f > \theta_a$ cannot occur. The equation for θ_y is redundant since θ_y is obtained from M_y and K_y. As described in the application, care has been taken in ensuring that K_y is always larger than $K_{40\%}$. The latter is used as an intermediate value between I and II stage stiffness, since the model is tri-linear. Finally, Haselton et al. (2008) provide also a marginal model for the parameter regulating cyclic degradation in the Ibarra model, i.e. the normalized total hysteretic energy $E_t/(M_y\theta_y)$.

The document provides also equations by Biskinis and Fardis (2010a, b), adopted since 2005 in earlier form in Eurocode 8 Part 3 (CEN 2005) and in latest fib Model Code (fib 2010), as well as by Zhu et al. (2007). These equations, however, are calibrated to provide cyclic values of the deformation thresholds, and their use is thus appropriate for LS identification when non-degrading models are used.

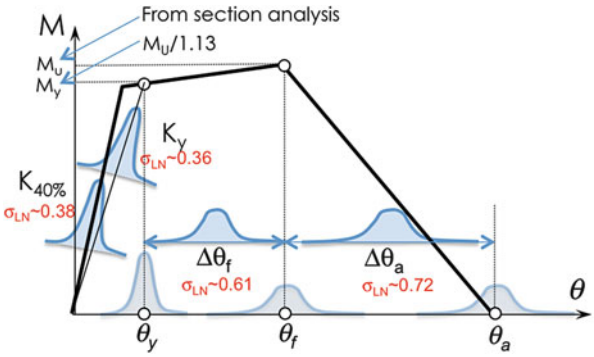

Fig. 3.9 Deformation limits for monotonic loading with schematic indication of the marginal PDF of each parameter

3.3.2.1 Biaxial Verification

Most response and all available capacity models are applicable for deformation in a single plane of flexure, while the document requires mandatory use of tri-dimensional models. While this does not represent a limitation for beams and for joints, with the exception of corner ones, columns are always subjected to biaxial deformation.

If degrading models are employed, currently the only option is to use the same model independently in the two orthogonal planes of flexure, disregarding interaction.

When non-degrading models are employed, interaction can be accounted for on the response side e.g. by use of fibre-discretized sections, and on the capacity side through the use of an "elliptical" rule for the evaluation of the local, member-level capacity-to-demand ratio (Biskinis and Fardis 2010a, b):

$$y = \sqrt{\left(\frac{\theta_2}{\theta_{2,LS}}\right)^2 + \left(\frac{\theta_3}{\theta_{3,LS}}\right)^2} \tag{3.17}$$

where θ_2 and θ_3 are the rotation demands in the two orthogonal planes, and $\theta_{2,LS}$ and $\theta_{3,LS}$ are the corresponding (cyclic) capacities for the LS under consideration.

3.4 Example Application to an RC Building

3.4.1 Premise

The document contains example applications to two real buildings, one in unreinforced masonry and the other in reinforced concrete. Together, the two examples illustrate the application of the three assessment methods presented in

the provisions: methods A and C with reference to the masonry building and method B with reference to the RC building.

The seismic risk assessment of the RC building has been carried out twice, using both non-degrading and degrading models, denoted as A and B, respectively. This has been done to provide users with an order of magnitude of the expected differences between the two approaches. Actually, the document provides results also for a third analysis with masonry infills, not reported here.

3.4.2 Description of the Structure

The building, shown in Fig. 3.10, is one of three blocks making up a school complex in southern Italy, built in the early 1960s. The structure consists of an RC space frame with extradosed beams and one-way hollow-core slabs, developing for three storeys over a sloping site. The lower storey is constrained since it is under-ground on three sides.

3.4.3 Seismic Action

For the purpose of the evaluation the building has been located at a site in the Basilicata region. Seismic hazard from the current design code, in terms of uniform hazard spectra at nine return periods, has been used to reconstruct median and fractile hazard curves at the first mode period of the structure (see later). The median curve has been interpolated with a quadratic polynomial in log-log space ($k_0 = 8.134 \times 10^{-5}$, $k_1 = 3.254$, $k_2 = 0.303$). Fractile curves have been used to compute a value of the hazard dispersion $\beta_H = 0.3$ (at a frequency between 1/500 and 1/1,000 years, close to the value of collapse MAF).

Thirty ground motion records have been selected from an aggregated database obtained merging the European Strong Motion database, and the Italian ITACA and SIMBAD databases. Records have been selected in the $M_w = [5.6;6.5]$ and $d_{epi} = [10\ km;30\ km]$ ranges (Fig. 3.11), centred around the values obtained from PSHA deaggregation in the same 1/500 and 1/1,000 years frequency range.

3.4.4 Preliminary Analysis and Test Results

No construction or design drawings were available. Based on an existing architectural survey, a structural survey was conducted to reconstruct the gross concrete frame dimensions. Based on these and on values for material properties, loads and reinforcement assumed based on the ruling design code at the time of construction a preliminary model was set–up (Fig. 3.12, where loads are shown in red, with height

Fig. 3.10 North-east view of the building

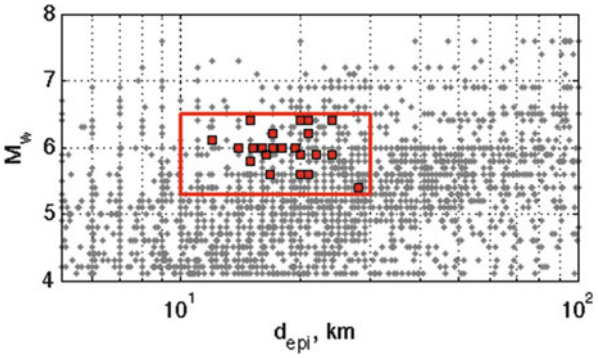

Fig. 3.11 Magnitude and distance bin used in the selection of recorded motions. Red dots indicate selected records

proportional to intensity). Modal analysis with full elastic response spectrum has provided the location where the largest inelastic deformation demand is expected. The most stressed columns are framed in red in Fig. 3.13, where actual members chosen for inspection and material sampling (at ground floor) are circled in blue. The results are reported in Table 3.2.

3.4.5 Structural Modeling

Structural analysis has been carried out using the general-purpose FE package OpenSees (McKenna et al. 2010). The behaviour of RC beam-column joints has not been modelled. Beams and columns have been modelled by means of elastic frame elements with zero length at the two ends, with independent uniaxial

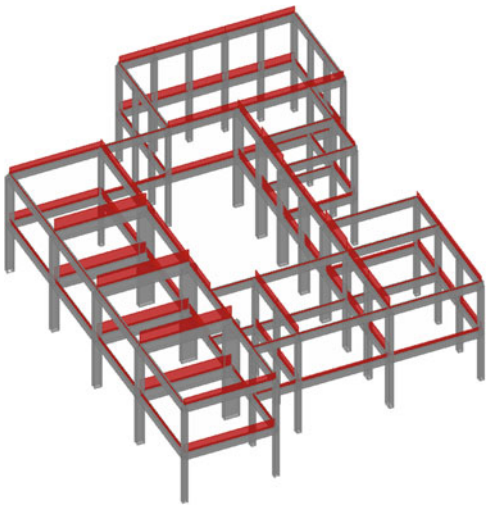

Fig. 3.12 View of preliminary analysis model with loads distributed to beams (one-way slabs)

constitutive laws on each degree of freedom.[1] The adopted moment-rotation law is the tri-linear one by Ibarra et al. (2005), in the implementation by (Lignos and Krawinkler 2012), and shown in Fig. 3.14 for the two orthogonal planes of flexure of one of the columns. Axial force-bending moment interaction is not included in the model, therefore a constant axial force needs to be assigned at the beginning of the analysis for determination of the model parameters. A single gravity load analysis on the median model has been used to determined axial forces in all columns, and these have been used for all random realizations of the structure (see next section).

Parameters for the Ibarra model have been predicted with the set of equations calibrated by Haselton et al. (2008). These equations include one that provides the degradation parameter:

$$\gamma = \frac{E_t}{M_y \theta_y} \tag{3.18}$$

Actually, the Opensees implementation of the Ibarra model requires in input the degradation parameter in the form:

$$\Lambda = \lambda \theta_p = \frac{E_t}{M_y \theta_p} \theta_p = \gamma \theta_y \tag{3.19}$$

Since method B has been used for the assessment (see later), a unique value of the degradation parameter needs to be assigned to the equivalent oscillator of each mode. The average value of Λ over the columns has been used.

[1] This option is easy to implement with a simple script in Tcl/Tk and is more robust than using a lumped plasticity element formulation, since it leaves complete control to the analyst through the global solution algorithm.

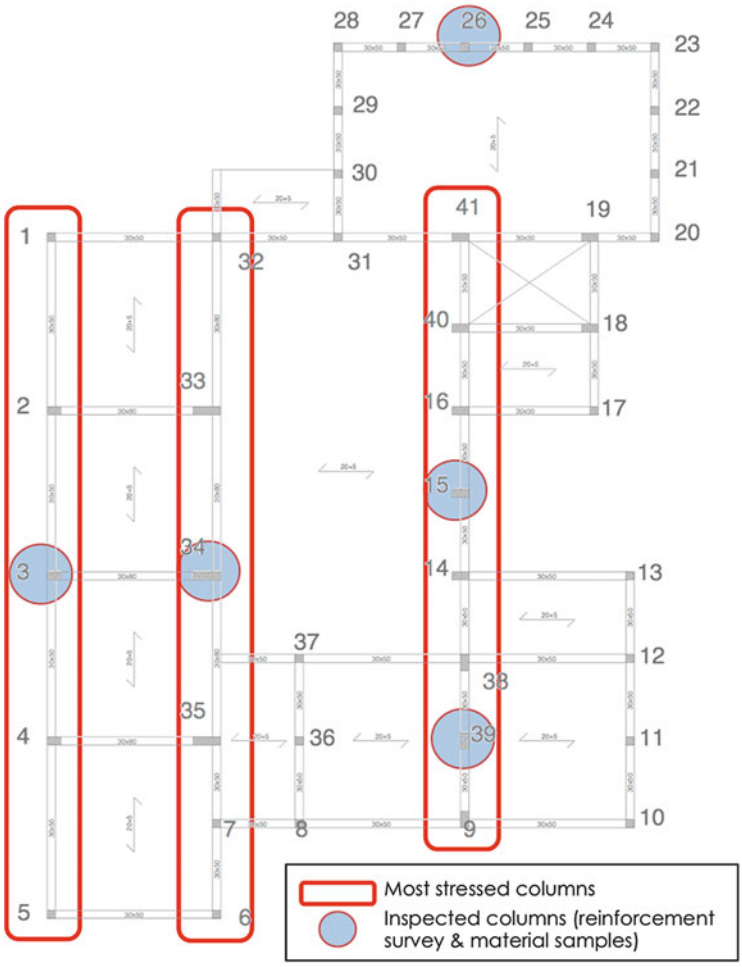

Fig. 3.13 Plan of inspections

As anticipated, the risk analysis has been performed twice, for both degrading and non-degrading models. In the latter case, for the sake of simplicity, the same Ibarra model has been used, but with zero, rather than negative, post-peak stiffness (e.g. M-θ curves in Fig. 3.14 go flat after 3.1 % and 3.2 %, respectively). Equation (3.6) has been used to check the collapse LS, and cyclic thresholds by Zhu et al. (2007) have been used for the ductile shear (θ_V) or flexural (θ_f) peak deformation. Each member has been attributed a ductile shear or flexural threshold based on the classification criterion proposed in Zhu et al., i.e. shear if geometric transverse reinforcement percentage lower or equal to 0.002, or shear span ratio lower than 2 (squat member), or plastic shear $V_p = 2M_u/L$ larger than 1.05 the shear strength (according to Sezen and Mohele 2002). Zhu et al. model for cyclic axial failure threshold θ_a has also been used for the non-degrading model.

Table 3.2 Results of tests on columns at ground floor

Member	B (mm)	H (mm)	Long. Reinf.	Transv. Reinf.	f_c (MPa)	f_y (MPa)
P3	300	500	6ϕ20	2ϕ6/200	16.7	–
P15	300	600	6ϕ20	2ϕ6/200	15.4	–
P26	300	300	4ϕ12	2ϕ6/200	17.8	–
P34	300	1,000	8ϕ20	2ϕ6/200	11.9	337
P39	300	500	6ϕ12	2ϕ6/200	11.6	370

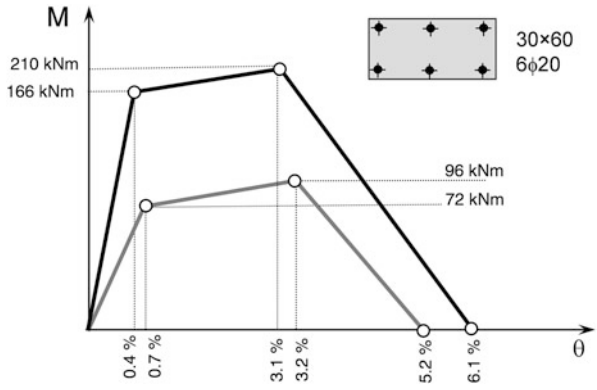

Fig. 3.14 Moment-rotation in two orthogonal planes

3.4.6 Uncertainty Modeling

In this application uncertainties that require analysis of alternative models, to be treated with the logic tree technique, have not been considered.

The uncertainties included in the assessment are:

- Material strengths: f_c and f_y, and ultimate concrete deformation ε_{cu}, which determine the constitutive law of the materials and enter into: (a) the stiffness of the elastic members, (b) section analysis leading to M_u, c) predictive formulas for deformation thresholds;
- Monotonic incremental deformation $\Delta\theta_f = \theta_f\text{-}\theta_y$ and $\Delta\theta_a = \theta_a\text{-}\theta_f$, and the cyclic degradation parameter γ, the latter two only for the degrading model;
- Cyclic deformation thresholds θ_f, θ_V and θ_a, for the non-degrading model;

All variables have been modelled as lognormal. As anticipated, statistical dependence of parameters within the same member or between same-parameter across different members has been modelled through assumed correlation coefficients.

In particular, in order to ensure that within each member $K_{40} > K_y$, perfect correlation has been assumed, a single standard normal random variable $\varepsilon_i \sim N(0,1)$ has been sampled in each member, and then amplified by the corresponding

Table 3.3 Distribution parameters for the random variables

RV	Median	Log-std	Correlation
f_c (MPa)	14.0	0.20	0.7
ε_{cu}	0.006	0.20	0.7
f_y (MPa)	338.0	0.10	0.8
K_{40}	Haselton et al.	0.38	0.8
K_y	Haselton et al.	0.36	0.8
$\Delta\theta_f$	Haselton et al.	0.61	0.8
$\Delta\theta_a$	Haselton et al.	0.72	0.8
θ_f	Zhu et al.	0.35	0.8
θ_V	Zhu et al.	0.27	0.8
θ_a	Zhu et al.	0.35	0.8
γ	Haselton et al.	0.50	0.8

logarithmic standard deviation to yield the factors $\exp(\varepsilon_i \sigma_{lnK40})$ and $\exp(\varepsilon_i \sigma_{lnKy})$ that multiply the corresponding medians.

Similarly, in order to avoid situations where a very ductile element loses axial bearing capacity prematurely, the variables $\Delta\theta_f$ and $\Delta\theta_a$ have been considered perfectly correlated and a single normal variable has been sampled as done for the stiffnesses.

Finally, in a way of simplicity, same-variables across different members (stiffnesses, deformation thresholds and material properties) have been considered equicorrelated, independently of distance (one could have used a distance-dependent correlation coefficient, with an exponential or squared exponential model, differentiating correlation lengths in the vertical and horizontal directions), with values reported in Table 3.3.

Figure 3.15 shows the moment-rotation law of a member for median values and one of the 30 samples of the random variables. The figure reports also in dashed line the non-degrading branch of the M-θ law, and the corresponding cyclic thresholds used for LS checking.

3.4.7 Method B and Response Analysis via Modal Pushover

The assessment has been carried out with method B, which uses IDA on equivalent oscillators obtained through nonlinear static analysis to characterize response. Several proposals are available in the literature for the determination of an approximate IDA curve starting from nonlinear static analysis, e.g. (Vamvatsikos and Cornell 2005; Dolsek and Fajfar 2005; Han and Chopra 2006). The latter, based on the modal pushover analysis (MPA) technique (Chopra and Goel 2002), has been chosen here due to its easy implementation with commercial analysis packages, since it uses invariant force patterns, and its applicability to general spatial geometries (Reyes and Chopra 2011). Differently from (Reyes and Chopra 2011), however, herein a single excitation that accounts for both orthogonal components of ground motion has been used. This excitation is derived as follows.

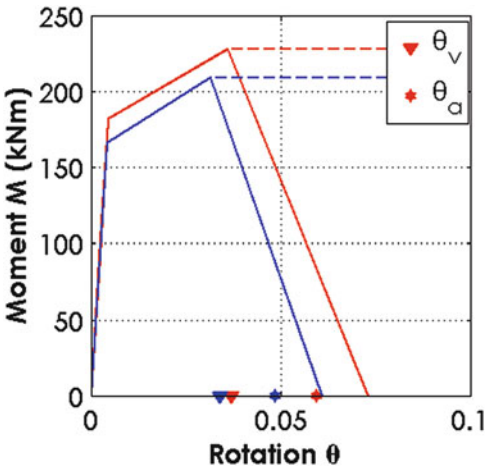

Fig. 3.15 Moment-rotation law for median values (*blue*) and one sample (*red*) of the random variables

The equations of motion for a discrete nonlinear MDOF system subjected to two components of ground motion along the X and Y axes are:

$$\mathbf{M}\ddot{\mathbf{u}} + \mathbf{C}\dot{\mathbf{u}} + \mathbf{F}(\mathbf{u}) = -\mathbf{M}(\mathbf{t}_X a_X + \mathbf{t}_Y a_Y) \tag{3.20}$$

with usual meaning of symbols and omitting the time dependence of input acceleration and response quantities. Adopting, according to the MPA method, the modal decomposition also in presence of nonlinear resisting forces, one gets:

$$M_i\ddot{q}_i + C_i\dot{q}_i + F_i = -(L_{iX}a_X + L_{iY}a_Y) \quad i = 1, \ldots, n \tag{3.21}$$

where $M_i = \boldsymbol{\phi}_i^{\mathrm{T}}\mathbf{M}\boldsymbol{\phi}_i$, $C_i = \boldsymbol{\phi}_i^{\mathrm{T}}\mathbf{C}\boldsymbol{\phi}_i$, $F_i = \boldsymbol{\phi}_i^{\mathrm{T}}\mathbf{F}$ is the projection of $\mathbf{F}$ on the i-th mode, and $L_{iX,Y} = \boldsymbol{\phi}_i^{\mathrm{T}}\mathbf{M}\mathbf{t}_{\mathrm{iX,Y}}$. Upon dividing (3.16) by the modal mass one gets:

$$\ddot{q}_i + 2\xi_i\omega_i\dot{q}_i + \frac{F_i}{M_i} = -(\Gamma_{iX}a_X + \Gamma_{iY}a_Y) \quad i = 1, \ldots, n \tag{3.22}$$

Finally, by further dividing (3.17) by the largest (dominant) of the two load participation factors L, e.g. that associated with the X component, one arrives at the equation of motion of a nonlinear oscillator having F/L-D force-displacement law, excited by an excitation which combines the two orthogonal input motions:

$$\ddot{D}_i + 2\xi_i\omega_i\dot{D}_i + \frac{F_i}{L_i} = -\left(a_X + \frac{\Gamma_{iY}}{\Gamma_{iX}}a_Y\right) \quad i = 1, \ldots, n \tag{3.23}$$

The assessment starts with modal analysis. For each significant vibration mode two nonlinear static analyses are carried out, one for each sign of the forces. The result of each nonlinear static analysis will consist of a database of local responses, i.e. matrices of nodal displacements, of size (n_{steps} x n_{nodes} x n_{dofs}), or of member

deformations, of size (n_{steps} x $n_{members}$ x $n_{deformations}$), plus a curve, usually called capacity curve, linking the base shear V_b to the displacement of a control degree of freedom u_c, usually taken to be that with the largest modal coordinate. The capacity curves are approximated by trilinear laws and transformed into *F*/*L*-*D* format. Each trilinear equivalent oscillator is then subjected to IDA with the 30 selected motions and local responses are obtained by interpolation of the corresponding database at the maximum displacement of the oscillator (for each motion and intensity level). Total responses are obtained from modal ones, at the same intensity S = s, by a suitable combination rule (SRSS or CQC). Based on total response, LS indicator functions Y are evaluated.

3.4.8 Results

Modal analysis of the median model (i.e. a model with median values assigned to all random variables) shows that the first three modes cumulatively account for more than 80 % of the total mass in both plan directions (Fig. 3.16). These mode shapes are the same for models A and B, since they have the same elastic properties.

These three modes are chosen for nonlinear static analysis. Figure 3.17, left, shows the corresponding results in terms of capacity curves with reference to model A. The figure shows also the tri-linear approximations of the curves used as monotonic backbone for the equivalent oscillators. The post-peak negative stiffness for this non-degrading model is entirely due to geometric effects (P-δ). Figure 3.17, right, compares the capacity curves for the three considered modes obtained with model A (red) and B (black), respectively. The curves depart from each other only after some excursion in the inelastic range, when the first local failure (exceedance of the ultimate/capping deformation) occurs. The total number of pushover analysis amounts to 2 signs × 3 modes × 30 models = 270, as shown in Fig. 3.18.

Figure 3.19 shows further details of the nonlinear static analysis, with the capacity curve of one of the 30 random realizations of Model B, subjected to modal forces according to its 3rd mode, in the positive sign, and the deformed shapes (same scale) at three steps corresponding to increasing levels of inelastic demand. The first and second step (S1 and S2 in the figure) correspond to the yield and peak displacement in the tri-linear approximation of the capacity curve, the last step S3 is midway between the peak and the last point. The deformed shapes report also the level of inelastic demand in plastic hinges, according to the convention already used in (Haselton and Deierlein 2007): hollow circles denote potential plastic hinge zones, blue and red circles denote inelastic demands lower and higher of the peak rotation, respectively. The diameter, for blue and red circles, is proportional to the D/C ratio. The blue circle fills completely the hollow black circle when $y = 1$ (Eq. 3.12), with $\theta_{LS} = \theta_f$ or θ_V. It can be observed that along the descending branch increases at some locations to more than three times the diameter of the black circle. This situation is numerically possible since the loss of axial load-bearing capacity is not modelled, and the analysis proceeds with redistribution

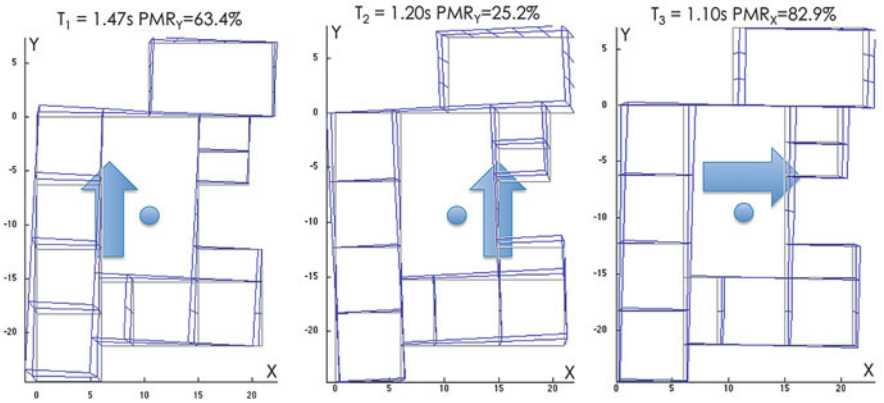

Fig. 3.16 Plan view of the first three mode shapes, with participating mass ratios in the dominant direction of each mode ("median" model)

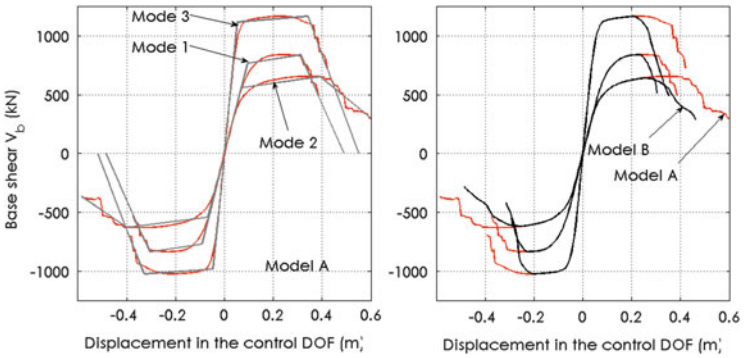

Fig. 3.17 Pushover curves for model A and B

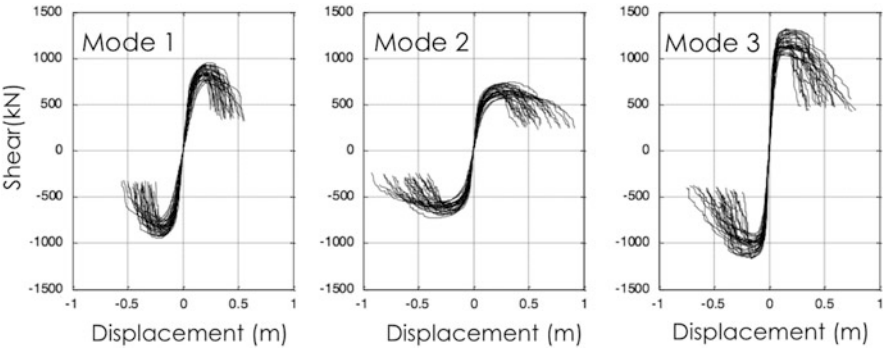

Fig. 3.18 Pushover curves of 30 random samples of model A

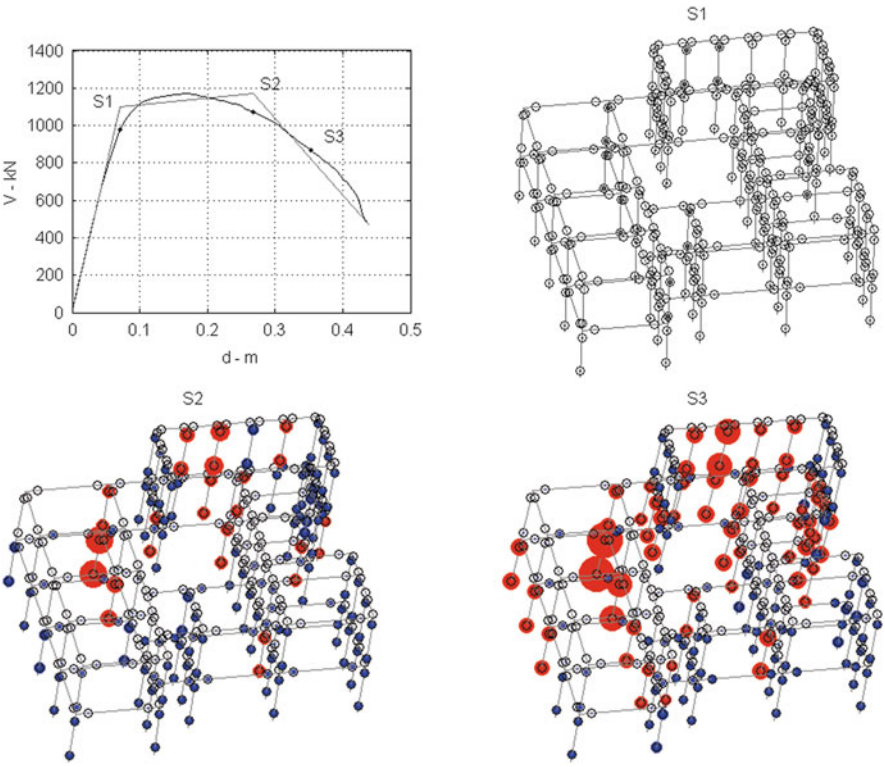

Fig. 3.19 Model B, Mode 3, pushover curve and deformed shapes at three different displacement levels, with indication of plastic hinge deformations (*hollow circles*, *blue circles* and *red circles* denote potential plastic hinges, active hinges before peak/ultimate deformation and hinges in the degrading post-peak branch, respectively)

of shear demand on the adjacent members. This fact, however, does not compromise the analysis since the axial collapse mode is actually checked a posteriori, using the θ_a model from Zhu et al. (2007) in conjunction with (3.8).

Figure 3.20 shows the response time-series for the equivalent oscillator (Model B, Mode 3, first random sample and associated motion) at three increasing intensity levels, shown below in terms of force-displacement loops. Depending on whether the largest response displacement has a positive or negative sign, the local responses at node/member level are interpolated from the database relative to the positive or negative pushover.

Finally, Figs. 3.21 and 3.22 show the IDA and the fragility curves for model A (left) and B (right), respectively. Green, blue and red dots on the IDA curves mark the attainment ($Y = 1$) of the damage, severe damage and collapse LS. Each cloud of points is used to determine the log-mean and log-standard deviation of the intensity leading to the corresponding LS: $S_{Y=1}$, parameters of the fragility curves reported below.

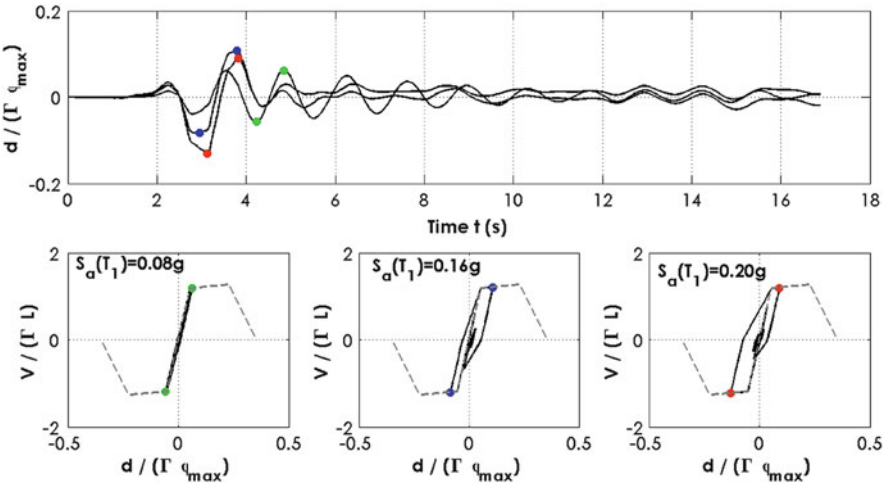

Fig. 3.20 Model B, Mode 3, response of the equivalent oscillator to the same motion at three increasing intensity levels (*top*) and corresponding force-deformation loops (*bottom*)

Convolution of the fragility curves in Fig. 3.22 with the hazard curve for the corresponding intensity measure, $S = S_a(T_1)$, yields the values of the mean annual rate of exceedance of the three LS's reported in Table 3.4. The table reports also the MAF thresholds for this school building (Class III structure, Table 3.1). As it can be seen, for the considered example the MAFs from the two modelling approaches are practically coincident for all LSs.

In conclusion, the example shows that the method is of relatively lengthy but rather straightforward application to real buildings, requiring in sequence a modal analysis, random sampling of model realizations, pushover analyses with invariant modal patterns, tri-linear approximation of capacity curves, expeditious IDA on equivalent SDOF oscillators, interpolation in the local response databases and CQC/SRSS combination, fragility parameters evaluation by simple statistical operations on the $S_{Y=1}$ intensity values. As long as MPA can provide a reasonable approximation of the dynamic response, Method B is a computationally effective alternative to Method A (IDA on complete model), since it requires determination and handling of much smaller response databases: where Method A requires determination of $n_{responses} \times n_{steps} \times n_{IM\text{-}levels}$ quantities per each record/model pair (with e.g. $n_{steps} = 2{,}000$ steps and $n_{IM\text{-}levels} = 10$), Method B requires determination of $n_{responses} \times n_{steps} \times n_{modes}$ quantities only (with e.g. $n_{steps} = 100$ steps and $n_{modes} = 3 \div 5$), since the IDA is carried out on a SDOF oscillator.

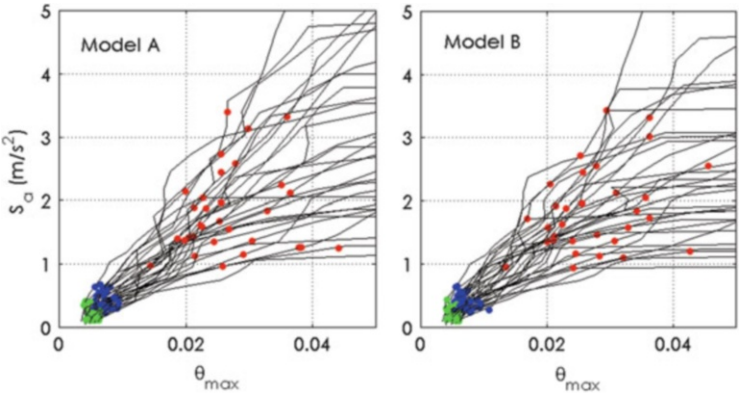

Fig. 3.21 IDA curves with indication of intensity leading to each LS for all records

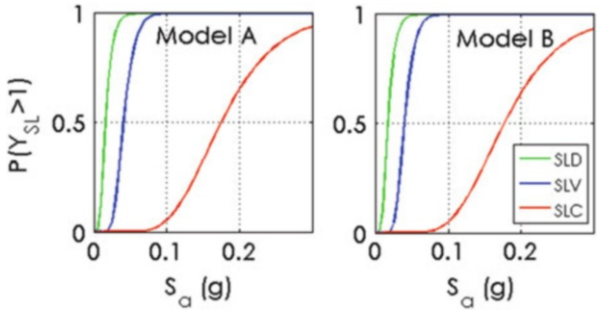

Fig. 3.22 Fragility curves

Table 3.4 Mean annual frequencies of LS exceedance for the two models and corresponding thresholds

Model	A	B	Threshold
λ_{SLD}	0.03150	0.03040	0.0300
λ_{SLS}	0.01270	0.01310	0.0032
λ_{SLC}	0.00119	0.00117	0.0015

3.5 Conclusions

The paper illustrates the latest Italian provisions issued by the National Research Council as Technical document 212/2013, for the probabilistic seismic assessment of existing RC and masonry buildings. These provisions are thought to overcome the limitations of the current normative, though they are not intended to replace them but, rather, to provide higher-level methods and tools for special applications and to inform possible revisions of the code in the future. The main merits of the document are:

(a) The systematic treatment of the problem of identification of global LS exceedance, in a manner consistent with their verbal description, with the introduction of LS indicator variables differentiated as a function of LS and modelling option.
(b) The explicit probabilistic treatment of all uncertainties, related to ground motion, material properties, modelling, geometry, detailing. In particular, the distinction of uncertainties that can be described within a single structural model via random variables and uncertainties that require the use of multiple models (logic tree) is introduced.
(c) The mandatory use of nonlinear analysis methods for response determination, and of ground motion time-series (preferably natural recorded) for the description of the seismic motion variability, irrespectively of the analysis method (dynamic or static).

Acknowledgements This paper focuses on the general part and on RC-specific provisions of the CNR-DT212 document, and includes an example application to a real RC building. Prof. Sergio Lagormarsino and Dr. Serena Cattari from University of Genoa have contributed to the drafting of the document, in particular for the masonry-specific provisions and application. The production of the document has been funded by Department of Civil Protection under the grant "DPC-Reluis 2010–2013" to the Italian Network of University Laboratories in Earthquake Engineering (ReLUIS).

References

Biskinis D, Fardis MN (2010a) Flexure-controlled ultimate deformations of members with continuous or lap-spliced bars. Struct Concr 11(2):93–108

Biskinis D, Fardis MN (2010b) Deformations at flexural yielding of members with continuous or lap-spliced bars. Struct Concr 11(3):127–138

Bradley B (2013) Ground motion selection for seismic risk analysis of civil infrastructure. In: Tesfamariam S, Goda K (eds) Handbook of seismic risk analysis and management of civil infrastructure systems. Woodhead Publishing Ltd, Cambridge. ISBN 978-0-85709-268-7

Chopra AK, Goel RK (2002) A modal pushover analysis procedure for estimating seismic demands for buildings. Earthq Eng Struct Dyn 31(3):561–582

Cornell C et al (2002) Probabilistic basis for 2000 SAC Federal Emergency Management Agency Steel Moment Frame Guidelines. J Struct Eng 128(4):526–533

Dolsek M, Fajfar P (2005) Simplified non-linear seismic analysis of infilled concrete frames. Earthq Eng Struct Dyn 34(1):49–66

Elwood K (2004) Modelling failures in existing reinforced concrete columns. Can J Civ Eng 31:846–859

fib, International Federation of Structural Concrete (2013) Model code for concrete structures 2010. Ernst & Sohn, Berlin. ISBN 978-3-433-03061-5

Han S, Chopra A (2006) Approximate incremental dynamic analysis using the modal pushover analysis procedure. Earthq Eng Struct Dyn 35:1853–1873

Haselton CB, Deierlein GG (2007) Assessing seismic collapse safety of modern reinforced concrete moment frame buildings, Blume center Technical report 156

Haselton CB, Liel AB, Taylor Lange S, Deierlein GG (2008) Beam-column element model calibrated for predicting flexural response leading to global collapse of RC frame buildings, PEER report 2007/03

Ibarra LF, Medina RA, Krawinkler H (2005) Hysteretic models that incorporate strength and stiffness deterioration. Earthq Eng Struct Dyn 34(12):1489–1511

Jalayer F, Franchin P, Pinto PE (2007) A scalar damage measure for seismic reliability analysis of RC frames. Earthq Eng Struct Dyn 36:2059–2079

Lignos D, Krawinkler H (2012) Sidesway collapse of deteriorating structural systems under seismic excitations. Blume Center technical report 177

Lin T, Haselton CB, Baker JW (2013) Conditional spectrum-based ground motion selection. Part I: hazard consistency for risk-based assessments. Earthq Eng Struct Dyn 42(12):1847–1865

McKenna F, Scott MH, Fenves GL (2010) Nonlinear finite-element analysis software architecture using object composition. ASCE J Comput Civ Eng 24(1):95–107

Pinto PE, Giannini R, Franchin P (2004) Seismic reliability analysis of structures. IUSS Press, Pavia. ISBN 88-7358-017-3

Reyes J, Chopra A (2011) Three dimensional modal pushover analysis of buildings subjected to two components of ground motion, including its evaluation for tall buildings. Earthq Eng Struct Dyn 40:789–806

Sezen H, Mohele JP (2004) Shear strength model for lightly reinforced concrete columns. ASCE J Struct Eng 130(11):1692–1703

Vamvatsikos D, Cornell CA (2002) Incremental dynamic analysis. Earthq Eng Struct Dyn 31 (3):491–514

Vamvatsikos D, Cornell C (2005) Direct estimation of seismic demand and capacity of multidegree-of-freedom systems through incremental dynamic analysis of single degree of freedom. J Struct Eng 131(4):589–599

Zhu L, Elwood K, Haukaas T (2007) Classification and seismic safety evaluation of existing reinforced concrete columns. J Struct Eng 133(9):1316–1330

(NTC2008) Ministero Infrastrutture, 2008. D.M.14/1/2008 “Norme Tecniche per le Costruzioni” (Testo integrato con la Circolare n°617/C.S.LL.PP. del 2/2/2009)

(EC8-3) Comité Européen de Normalisation (2005) Eurocode 8: design of structures for earthquake resistance – Part 3: assessment and retrofitting of buildings